Catalysis Communications 172 (2022) 106547

Contents lists available at ScienceDirect

Catalysis Communications

journal homepage: www.elsevier.com/locate/catcom

PGM nanoparticle-based alumina aerogels for three-way catalyst applications

Ann M. Anderson [a,*], Bradford A. Bruno [a], Joana Santos [a], Patrick J. Barry [b], Mary K. Carroll [b]

[a] Department of Mechanical Engineering, Union College, Schenectady, NY 12308, USA
[b] Department of Chemistry, Union College, Schenectady, NY 12308, USA

ARTICLE INFO

Keywords:
Aerogel catalysts
Three-way catalysts
Platinum
Palladium
Rhodium

ABSTRACT

Alumina aerogels doped with PGM nanoparticles are prepared and characterized as candidates for three-way catalysts (TWCs). After heat-treatment at 800 °C the materials maintain low density (~0.1 g/mL), high surface area (290–460 m^2/g) and high pore volume (1.4–3.6 g/m^3), but show some agglomeration of the nanoparticles. Pt-, Pd- and Rh-alumina aerogels show TWC activity comparable to a commercial catalyst. Light-off temperatures for CO and propene by Pd/Al_2O_3 aerogels are 190 and 220 °C (respectively) while for NO by Rh/Al_2O_3 aerogel is 250 °C. These materials are loaded at 0.08–0.16 g/L (2–3 g/ft^3), considerably lower than typical TWC PGM loadings of 1.8–2.8 g/L (50–80 g/ft^3).

1. Introduction

Aerogels' unique blend of physical and chemical properties makes them potentially advantageous for catalytic conversion of the harmful emissions from gasoline engines that are a major source of air pollution. In gasoline engine automotive applications, pollutants, such as nitrogen oxides (NOx), carbon monoxide (CO) and unburned hydrocarbons (HC), are removed by "catalytic converters" (better known as three-way catalysts, TWCs), that convert these pollutants into less harmful species. TWCs are generally composed of a ceramic (cordierite) honeycomb structure wash-coated with a high-surface-area, thermally stable, inorganic oxide material onto which catalytic species (e.g. platinum group metals, PGMs) have been dispersed. The resulting catalytically coated honeycomb "core" is placed in a metal housing (often referred to as the "can") to contain the exhaust flow, protect the fragile core from the elements and facilitate attachment to the rest of the automotive engine exhaust system. The washcoat also serves to physically separate the PGMs and prevent agglomeration, sintering or other unwanted interactions. Washcoat materials include oxides such as Al_2O_3, SiO_2, TiO_2, CeO_2, ZrO_2, V_2O_5, and La_2O_3 [1]. In addition to providing a support for the catalysts, some of these materials are added to the washcoat as promoters or stabilizers, and some exhibit catalytic activity of their own.

Due to the high cost of PGMs (monetary and environmental), methods for reducing PGM use are sought [2–4]. The use of aerogel-based catalysts in TWCs provides one such potential method. Many aerogel properties are desirable for TWCs. Stability at high temperature could reduce diffusion and sintering of PGM active sites, allowing the TWC to be placed closer to the engine, thereby reducing the time needed for the TWC to reach operating temperature and "light-off." Light-off temperature is defined as the temperature at which 50% of the target pollutant is converted (this is also often referred to as T_{50} in the literature). High surface area of the aerogel could result in more catalytically-active sites and improve gas/solid interaction. Finally, the ability to tailor aerogel chemistry through the sol-gel process allows for the production of many types of catalytic aerogel materials. The use of aerogels as catalysts in the treatment of both water and air pollution applications has been well documented in several review articles [5–7]. To the best of our knowledge the development of aerogel catalysts by other research groups has focused on their use in single reactions as opposed to the challenge posed by the needs of a TWC (simultaneous conversion of CO, NOx and HCs).

Our group has taken two approaches to preparing catalytic aerogels for automotive pollution mitigation: (1) combining different precursor chemicals to make mixed-metal aerogels and (2) incorporating metal nano- or microparticles into the aerogel precursor mixture. Alumina forms the basis of the industry standard washcoat so we have used alumina aerogel as our support structure for the catalytic aerogels. We have performed studies of plain alumina aerogel [8] up to 1100 °C [9]. TWC characterization of the alumina aerogel was poor and it was clear that doping with another metal would be needed. To date, we have

* Corresponding author.
E-mail address: andersoa@union.edu (A.M. Anderson).

https://doi.org/10.1016/j.catcom.2022.106547
Received 30 August 2022; Received in revised form 20 October 2022; Accepted 23 October 2022
Available online 25 October 2022

focused on the production of non-PGM-based aerogels for TWC activity including copper-alumina [10–12], nickel-alumina, ceria-alumina [13] and chromia-alumina [14] aerogels. These materials show TWC activity but don't generally light off until ~250 °C, which is higher than light-off temperatures achieved with traditional TWC washcoats with PGMs. Recently we have shifted to using aerogels as a carrier for PGM materials with the hypothesis that, although the mechanisms for catalytic reaction would presumably be the same for PGMs on alumina aerogel as on other alumina supports, smaller amounts of PGMs may be required due to the aerogel's properties and structure.

PGM-based aerogels can be synthesized using a variety of methods. They can be made through a co-precursor method in which a PGM-containing solution [15–17] or PGM nanoparticles [18] are added directly to the aerogel precursor mixture before gelation. Alternatively, the PGM material can be introduced to an already formed wet-gel via an impregnation method involving solvent exchange with a PGM-containing compound in an aging solvent [19,20]. The aerogel can also be doped via supercritical deposition onto the surface [21] or impregnation via a solvent containing the PGM [22].

Sanz-Moral et al. [18] examined the performance of Pd-silica aerogels prepared via three methods: (1) impregnation by adding $Pd(acac)_2$ to the wet-gel aging solvent prior to supercritical extraction, (2) a co-precursor method by suspending metallic Pd nanoparticles in the wet gel solvent (methanol) and (3) supercritical deposition on the aerogel using $Pd(acac)_2$ in CO_2. The supercritical deposition methods reduced surface area by 2% and pore volume by 21% compared to an undoped silica aerogel, whereas the co-precursor method with nanoparticles resulted in the largest reduction in surface area and pore volume (9% and 41% respectively). They found evidence of particle agglomeration in the materials prepared via the co-precursor method with nanoparticles and showed that the catalytic activity for hydrogenation of D-glucose was best with the aerogels prepared via the impregnation method.

Here, we describe PGM-containing alumina aerogel materials with activity as three-way catalysts. These materials are prepared with low PGM loading via a novel scalable aerogel fabrication method, characterized using a barrage of standard techniques, and tested against simulated automotive exhaust under dry and humid conditions. Due to ease of fabrication, in this first study of the TWC performance of PGM-containing aerogels we have focused on a preparation method that utilizes suspensions of PGM nanoparticles that are easily added to the aerogel precursor solution as demonstrated in our earlier work with copper nanoparticles [23]. This study extends our previous work with non-PGM-based catalytic aerogels.

2. Experimental

2.1. Materials

We used aluminum chloride hexahydrate, $AlCl_3 \bullet 6H_2O$ (99%) and propylene oxide (>99%) sourced from Sigma-Aldrich. Denatured (reagent-grade) ethanol and absolute ethanol (200 proof) were sourced from Fisher Scientific. Platinum, palladium and rhodium nanoparticles (99.95%, 15 nm) were acquired from US Research Nanomaterials, Inc., as 1000-ppm dispersions in ethanol.

2.2. Wet-gel preparation

The PGM-alumina wet-gels were prepared using an epoxide-assisted co-precursor method [24]. First, we dissolved 2.95 g of aluminum chloride hexahydrate in a covered beaker in 10 or 15 mL of denatured ethanol using a magnetic stirrer. This typically took <1 h. While stirring, 5 or 10 mL (so that the total volume of ethanol plus suspension = 20 mL) of one of the nanoparticle dispersions (either Pt, Pd or Rh) was added to the salt solution followed by 4.25 mL of propylene oxide (added using a syringe). After about 5 min, the solution gelled and the beaker was removed from the stir plate, sealed with paraffin film and left in a hood. After 24 h, the wet gel was broken up into small (<1 cm) pieces and 20 mL of absolute ethanol was added to the beaker. The solvent was exchanged two more times in 24-h intervals to remove the propylene oxide [9]. In total, the wet-gel preparation took approximately four days.

2.3. Aerogel synthesis

Pieces from three separate wet-gel batches were placed in an 8.1-cm diameter well of a 12.7 × 12.7 × 1.9 cm 416 stainless steel mold and covered with absolute ethanol before processing. A Tetrahedron 24-ton MTP-14 hydraulic hot press was used to supercritically extract the ethanol via the RSCE method developed by Union College [25–27], to yield Pd-, Pt-, or Rh- containing alumina aerogels. For the supercritical extraction the hot press used a restraining force of 200 kN and a heating and cooling rate of 2.5 °C/min. The supercritical extraction step took about 5.5 h.

2.4. Heat treatment

After processing, the aerogel samples were placed in loosely covered ceramic crucibles in a programmable furnace (Thermo-Scientific Thermolyne) for calcining. Samples were heated to 800 °C, held at that temperature for 21–24 h, then cooled to room temperature, all under ambient pressure.

2.5. Characterization methods

Density was estimated from mass and volume measurements of the aerogel pieces. Because the aerogel pieces are on the order on 1–2 mm the volume measurement is overestimated resulting in an underestimate of the bulk density.

Surface area and pore distributions were acquired using nitrogen gas adsorption (Micromeritics ASAP 2020). Samples were prepared by gently crushing 0.1–0.2 g of material to a coarse powder and then degassing it at 90 °C for 2 h and 200 °C for 6 h. The BET surface area was determined using partial pressures from 0 to 0.3. BJH pore distributions were determined using the desorption isotherm. Equilibration times of 20–50 s were used to avoid the effects of pore compression at high partial pressures [28].

Powder X-ray diffraction patterns of select samples were acquired using a Rigaku Powder SE X-ray diffractometer with a copper X-ray source tube and nickel filter. Samples were crushed into a fine powder and pressed into the 0.5-mm well of a glass sample holder. Signal was collected over a 2θ range of 5–80° using a 1° incident slit, a 20-mm receiving slit, a step size of 0.01° and at a speed of 2.5°/min. Patterns were analyzed using the Rigaku Smart Lab Studio II software.

For scanning electron microscopy (SEM) imaging, samples were prepared by pressing aerogel powder into SEM stage pins covered in double sided carbon tape. No additional preparation was used (aerogels were imaged uncoated). A Zeiss EVO MA-15 SEM was used to image the aerogel powders using a working distance of 7–8 mm, accelerating voltages of 10–15 kV and a spot size of 390. Energy dispersive X-ray (EDX) maps were obtained with a Bruker XFlash 6 | 30 detector coupled to the SEM instrument. Topographical images were obtained using backscattered electron (BSE) detection, and no image filter was used. Oxygen, aluminum, platinum, palladium and rhodium maps were imaged with signal collected for 10 min for each map.

2.6. Catalytic testing

The catalytic testing methods used are identical to those described fully in earlier work [12] but certain salient details are repeated here for the convenience of the reader. The catalytic tests were performed using the Union Catalytic Aerogel Testbed (UCAT, shown schematically in

Supplemental Fig. S1). Additional detail on the design and capabilities of UCAT are provided in the supplement and in Bruno et al. [29].

For each catalytic performance test approximately 22 mL (2 g) of lightly crushed heat-treated aerogel sample, in the physical form shown in Supplemental Fig. S2 (i.e. ranging from small pieces, ca. 1–5 mm, to coarse powders), is loaded into each of UCAT's two identical test sections. The test sections are then placed inside the furnace (ThermCraft 9800 W Split Tube), and tests were run at 25 °C increments from 150 to 200 °C, and then at 50 °C increments from 200 to 450 °C.

Sample gas consisting of 970–1183 ppm HC, 970–1183 ppm NO, 0.49–0.56% CO, 0.17–0.2 H_2, 12.63–15.4% CO_2, 0 or 13% H_2O, 0.12 or 1.15% O_2 with the balance N_2 (see Table S1 for details) is fed to the system. Commercial five-gas analyzers (Infrared Industries FGA4000XDS 5 Gas Analyzer, one per test section) are used to measure the concentrations of CO, NO and HC. The gas flow rate is maintained at a constant space velocity of 17 s^{-1} (61,200 h^{-1}) in the sample for all tests. Concentration measurements are taken after the gas passes through either the aerogel sample for treatment or through a bypass line and emerges untreated. The percent conversion for each pollutant is calculated by comparing the treated concentration to the untreated (bypass) concentration. This procedure corrects for potential slight differences in calibration between and/or drift in sensitivity of the two five-gas analyzers. However, a slight zero offset error on the output of one of the five-gas analyzers remained and required additional correction (i.e. average offset subtraction) when processing the raw data.

In testing, the aerogel catalysts were exposed to four different test gas blends (see Table S1), identical to those used in Anderson et al. [12]. The test blends and testing conditions are all based on recommendations from CLEERS (Cross-Cut Lean Exhaust Emissions Reductions Simulations) [30], with some modifications required by our equipment as discussed in Anderson et al. [12]. The "Stoichiometry Number, S", as described by Schlatter [31] for each gas blend is calculated as:

$$S = \frac{2O_2 + NO}{CO + H_2 + 3nC_nH_{2n} + (3n+1)C_nH_{2n+2}}$$

and indicates a gas mixture's propensity to favor oxidation or reduction reactions. S numbers >1 indicate a gas blend that would favor oxidation reactions, as would typically be produced from "fuel lean" or "excess air" gasoline combustion (relative to stoichiometric), whereas S numbers lower than 1 indicate exhaust that would favor reduction reactions typically produced from "fuel rich" gasoline combustion. As such S can provide some level of insight when comparing test results between studies using different gas blends. Further discussion of the motivation in selecting test blends is available in the supplemental materials.

3. Results and discussion

3.1. PGM loading

The aerogels prepared with 5 mL of the nanoparticle solution resulted in heat-treated materials that contain 0.8% by mass of PGM material (assuming no loss of PGM during fabrication, processing or heat-treatment). Given a bulk density of approximately 0.1 g/mL for the heat-treated aerogels this results in a loading of 0.08 g/L (2.3 g/ft^3). The aerogels prepared with 10 mL of the nano-particle solution resulted in materials containing 1.6% by mass of PGM material, corresponding to a loading of 0.16 g/L (4.6 g/ft^3). Samples will be known as 0.8% Pt/Al_2O_3, 0.8% Pd/Al_2O_3, 0.8% Rh/Al_2O_3 and 1.6% Pd/Al_2O_3. The aerogel PGM loadings, when reported in this way, most nearly map onto PGM per unit volume of "washcoat" (often called "washcoat loading") and care must be taken when making comparisons to the literature because PGM loadings are often presented as "can loadings" of mass of PGM per total volume of the finished TWC unit (including the empty space in the honeycomb structure's flow passages).

Supplemental Fig. S2 shows images of the 0.8% Pt/Al_2O_3, 0.8% Pd/Al_2O_3, and 0.8% Rh/Al_2O_3 materials before RSCE processing, after RSCE processing and after heat treatment. Of note is the lack of any significant shrinkage during the supercritical extraction. It is possible to identify specific wet or dry pieces pre- and post-RSCE processing. However, significant shrinkage occurs upon heat treatment, which is consistent with previous work with alumina-based aerogels [9–12]. We also see that the aerogels change colour after processing and heat treatment, indicative of structural changes.

3.2. Density surface area and pore distribution

Table 1 presents density, surface area and pore volume results for the PGM-based aerogels in the as-prepared form and after heat treatment. The density of the as-prepared materials is 0.05–0.06 g/mL and after heat treatment it increases to about 0.1 g/mL. The increase in density is due to sintering that occurs during heat-treatment and is typical of what we see with other alumina-based aerogels [9–12].

The surface area of the as-prepared materials made from the recipes containing 0.8% PGM is about 10% lower than the materials prepared without PGMs (650 vs 730 m^2/g), although that difference is just within the uncertainty of the measurements. The samples prepared with 1.6% PGM have a 40% lower surface area (420 m^2/g). After heat treatment the 0.8% Pt/Al_2O_3 and 0.8% Pd/Al_2O_3 aerogels have surface area similar to that of the heat-treated alumina aerogel (~410 m^2/g), all showing a reduction in surface area of about 30%. The 0.8% Rh/Al_2O_3 aerogel surface area is decreased by about 50% after heat treatment (290 m^2/g). This is a significantly smaller decrease in surface area after heat treatment than what we have measured with copper-alumina aerogels prepared via an impregnation method. An as-prepared copper-alumina aerogel has a surface area ~350 m^2/g, after heat treatment surface area is reduced by about 80% to ~65 m^2/g [10,12]. Adding copper nanoparticles to silica aerogel lowered surface area by 40–80% from about 500 m^2/g to 300–100 m^2/g (depending on the size and amount of nanoparticles) [23]. These aerogel surface area values are considerably larger than those reported for a standard alumina washcoat [32], which had a surface area of about 300 m^2/g (as prepared) and about 200 m^2/g after 4 h of heat treatment at 800 °C. Theis et al. found that addition of 0.14–4 wt% Pd to the standard alumina washcoat did not have a significant effect on the surface area [32].

All of the as-prepared aerogel samples have very high pore volume (4–7.5 cm^3/g), which we note can only be detected using a 50-s equilibration time with tests taking 60–80 h. The results reported in Table 1 are calculated from the desorption isotherm; however, the values calculated from the adsorption isotherm are essentially the same. The aerogels prepared with platinum nanoparticles show significantly reduced pore volume compared to the plain alumina aerogel, whereas the lower concentration (0.8%) of Pd and Rh nanoparticles is not observed to significantly affect the pore volume. Heat treatment decreases pore volume, as expected.

Fig. 1 plots BJH pore distributions derived from the desorption isotherm for the as-prepared samples (1a) and heat-treated samples (1b). For the as-prepared materials the peak pore volume occurs at about 30 nm for the alumina aerogel and the peak has lower pore volume and is shifted to about 40 nm when nanoparticles are added. We saw a similar trend when we added copper nanoparticles to silica aerogels [23]. After heat treatment the peak pore volume for the alumina aerogel occurs at about 40 nm and is shifted to about 50 nm when nanoparticles are added.

3.3. SEM images/EDX maps

Both because of the small size of the nanoparticles employed (15 nm) and the difficulty associated with imaging highly insulating material, SEM is of limited utility in the characterization of the PGM-doped aerogels. EDX provides some information regarding aerogel composition and evidence of PGM nanoparticle agglomeration. Here, we present

Table 1
Density, Surface Area and Pore Volume.

	Density (g/mL)		Surface Area (m^2/g)		Pore Volume (cm^3/g)	
	As-prepared	Heat Treated	As-prepared	Heat Treated	As-prepared	Heat Treated
Al_2O_3	–	–	730 ± 50	410 ± 20	7.5 ± 0.5	4.9 ± 0.2
0.8% Pt/Al_2O_3	0.06	0.10	630 ± 40	420 ± 40	4.3 ± 0.3	3.6 ± 0.3
1.6% Pt/Al_2O_3	0.06	0.10	510 ± 30	–	3.7 ± 0.2	–
0.8% Pd/Al_2O_3	0.05	0.10	660 ± 40	460 ± 30	7.8 ± 0.5	2.1 ± 0.2
1.6% Pd/Al_2O_3	0.06	0.09	420 ± 20	300 ± 20	4.1 ± 0.2	2.2 ± 0.1
0.8% Rh/Al_2O_3	0.05	0.11	650 ± 50	290 ± 20	6.6 ± 0.5	1.4 ± 0.1

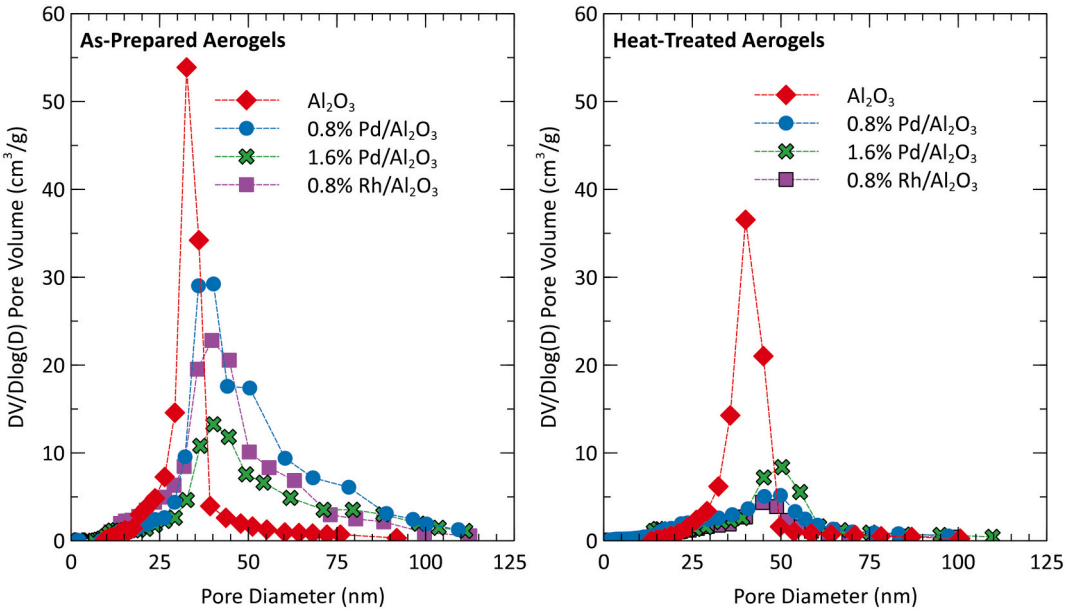

Fig. 1. BJH pore distributions for as-prepared (left) and heat-treated (right) alumina aerogels (red diamonds), 0.8% Pd/Al_2O_3 aerogels (blue circles), 1.6% Pd/Al_2O_3 aerogels (green crosses) and 0.8% Rh/Al_2O_3 aerogels (purple squares). (For interpretation of the references to colour in this figure legend, the reader is referred to the web version of this article.)

representative data.

The as-prepared 0.8% Rh/Al_2O_3 aerogel SEM images show the typical "fluffy" aerogel structure often observed for aerogels (see Supplemental Fig. S3a). The EDX maps show a fairly uniform dispersion of Al and O, consistent with an amorphous alumina structure. Rh is also dispersed throughout; however, there is evidence of some agglomeration, with Rh clusters as large as 10 μm in diameter (see Supplemental Fig. S3b-e).

Fig. 2 presents SEM/EDX images of a heat-treated 1.6% Pt/Al_2O_3 aerogel. As is the case for all of the PGM-doped aerogels, the overall structure is observed to be amorphous. The EDX map shows a uniform distribution of Al and O throughout the matrix, along with some 3–5 μm clusters of Pt and a few smaller (~500 nm) Pt clusters. Overall, although it is difficult to detect individual nanoparticles using the SEM/EDX, the

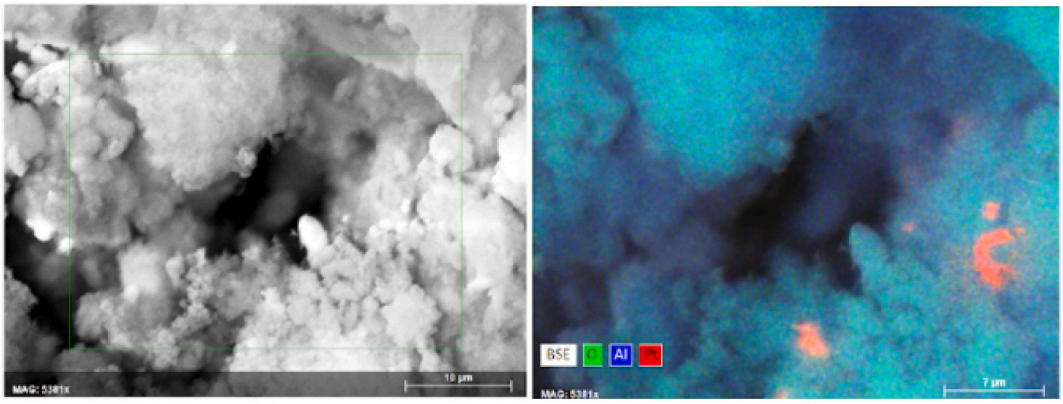

Fig. 2. SEM and EDX images of a heat-treated 1.6% Pt/Al_2O_3 aerogel: (a) SEM image (10-μm scale bar; green rectangle indicates area chosen for EDX imaging), (b) EDX maps for Al (blue), O (green) and Pt (red) overlaid on the backscattered electron image (scale bar 7 μm). (For interpretation of the references to colour in this figure legend, the reader is referred to the web version of this article.)

results confirm the presence of PGMs in the aerogels and indicate that some agglomeration occurs.

3.4. XRD patterns

Although aerogel materials are largely amorphous, powder XRD can be used to detect and identify microcrystalline components within the aerogel matrix. The as-prepared aerogels show peaks (see Supplemental Fig. S4) indicative of boehmite (15°, 28°, 49° and 65° ICDD PDF-2 card 01–074-2895), which is consistent with previous work with alumina-based aerogels [10,12]. The pattern for the aerogel containing Rh is identical to that of the plain alumina aerogel (as is the pattern for the as-prepared 0.8% Pt/Al_2O_3 and 0.8% Pd/Al_2O_3 samples, not shown) with no peaks corresponding to the added PGM nanoparticles. This result was expected due to the small size and low concentration of the nanoparticles employed. After heat treatment in air the alumina aerogel (see Supplemental Fig. S4) shows peaks corresponding to γ-alumina (19°, 32°, 37°, 45.5°, 60°, 66° ICDD PDF-2 card 00–050-0741). In addition to the γ-alumina peaks, the 0.8% Rh/Al_2O_3 pattern contains small peaks (just detectable) corresponding to Rh_2O_3 (33.2°, 34.4°, 48.7°, 61.7° ICDD PDF-2 card 01–073-0168). The formation of rhodium-oxide species under high-temperature oxidizing conditions is consistent with prior work by Hwang et al. [33], among others.

Fig. 3 compares the XRD patterns of the three different PGM nanoparticle-based aerogels after heat treatment. In addition to the peaks attributed to γ-alumina, there are sharp peaks corresponding to crystalline PdO (34°, 42°, 55°, 60°) in the 1.6% Pd/Al_2O_3 aerogel and to Pt (39.7°, 46.2°, 67.4°, ICDD PDF-2 card 00–070-2431) in the 0.8% Pt/Al_2O_3 aerogel. These XRD patterns demonstrate convincingly that PGM materials have been successfully entrapped in the aerogel matrix. They also indicate that, at least for the Rh and Pd nanoparticles, changes in oxidation state occur under the heat-treatment conditions employed. XRD is not a particularly sensitive method, so the fact that these peaks are detected not only demonstrates that some structural changes occur during heat-treatment but might also be an indication that these structural changes are associated with agglomeration of the nanoparticles.

3.5. Catalytic test results

The catalytic testing results for aerogels containing a single type of PGM nanoparticle (Pd, Rh or Pt) are presented in Fig. 4 (0.8% Pd/Al_2O_3 and 1.6% Pd/Al_2O_3), Fig. 5 (0.8% Rh/Al_2O_3) and Supplementary Fig. S5 (0.8% Pt/Al_2O_3). Each figure includes plots for the percent conversion of HC, CO and NO versus average test cell temperature. The three plots on the left represent high O_2 conditions and the three on the right represent low-O_2 conditions. Each plot shows results for dry (D) exhaust and humid (H) exhaust. In the following discussions most focus is placed on the oxidizing response (i.e. removal of CO an HC) under the conditions most favorable for oxidation (i.e. high-O_2 / S number >1) and the reduction response (removal of NO) under conditions most favorable for reduction (i.e. low-O_2 / S number lower than 1). These are the top two plots in the left column and bottom plot in the right column of each figure.

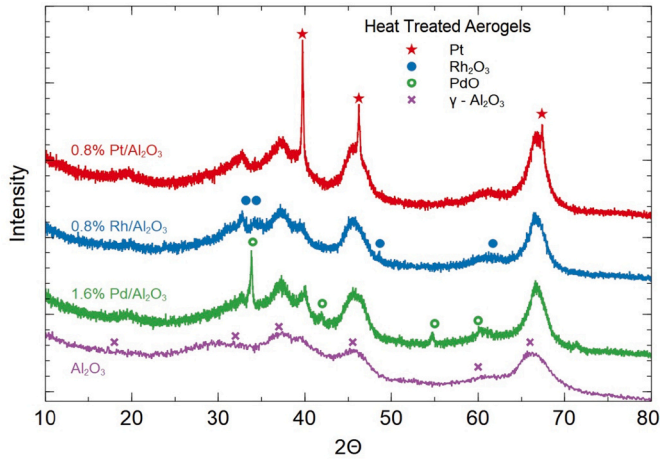

Fig. 3. XRD Patterns of 0.8% Pt/Al_2O_3 (red), 0.8% Rh/Al_2O_3 (blue), a 1.6% Pd/Al_2O_3 (green), and plain alumina (purple) aerogels. All samples were heat treated and the 0.8% Pt/Al_2O_3 sample had also been catalytically tested. Peaks corresponding to platinum (red stars), rhodium(III) oxide (blue filled circles), palladium(II) oxide (green open circles) and γ-alumina (purple crosses) are marked. (For interpretation of the references to colour in this figure legend, the reader is referred to the web version of this article.)

The light-off temperatures for the 0.8% Pt/Al_2O_3 aerogels are relatively high (see Supplemental Fig. S5). The light-off temperatures for CO and HC are 400–450 °C (high-O_2 conditions) and over 500 °C for NO (low-O_2 conditions). Conversion of CO and HC is improved in the presence of humidity, whereas the conversion of NO is suppressed in the presence of humidity. Under high-O_2 conditions there is no conversion of NO, and under low-O_2 conditions there is no conversion of CO and little conversion of HCs. For the dry exhaust tests, each data point represents the average for two separate samples, each tested three times with the error bars representing one standard deviation in that data. Under the humid conditions one test was performed on a single sample. Because of the relatively poor performance (i.e. high light-off temperature and relatively low catalytic activity toward NO) of the 0.8% Pt/Al_2O_3 aerogel material, we did not perform catalytic testing of the 1.6% Pt/Al_2O_3 aerogel.

We observed much better performance for the Pd/Al_2O_3 aerogels, as seen in Fig. 4, with light-off temperatures as low as 225 °C for HC (high-O_2) and 190 °C for CO (high-O_2). Under low-O_2 conditions the NO light-off temperatures are above 400 °C. There is little difference in performance between the dry and humid exhaust conditions for HC and CO in high-O_2 conditions, whereas the NO performs moderately better under dry-exhaust conditions in low-O_2 conditions at temperatures up to 350 °C. Above 350 °C the NO conversion is better in the humid conditions. We do not have a fundamental explanation for this unanticipated result and have not explored it further because under all conditions tested the NO conversion is too low to be of interest for TWC applications. The 1.6% Pd/Al_2O_3 aerogel might perform slightly better than the 0.8% Pd/Al_2O_3 aerogel; however, that difference is within the scatter in the measurements. In these plots, each data point represents the average for two separate samples (0.8% Pd/Al_2O_3) or a single sample (1.6% Pd/Al_2O_3) undergoing at least two tests. The error bars represent one standard deviation.

Fig. 5 summarizes the performance of the 0.8% Rh/Al_2O_3 aerogel. The light-off temperatures for HC and CO under high-O_2 conditions (240–275 °C for HC and 240 °C for CO) are higher than those for the 0.8% Pd/Al_2O_3 aerogel but lower than those for the 0.8% Pt/Al_2O_3 aerogel. However, under low-O_2 conditions the 0.8% Rh/Al_2O_3 aerogel had a light-off temperature of about 245 °C for NO. In addition, there is some conversion of the NO by the 0.8% Rh/Al_2O_3 aerogel under high-O_2 conditions, which was not seen with the Pt/Al_2O_3 or Pd/Al_2O_3 aerogels. The increased performance for NO conversion was anticipated as Rh is often included in TWC catalyst formations, despite its high price, specifically because it is effective against NO. Furthermore, under both dry and humid conditions at the temperatures experienced in UCAT, evidence of thermal deactivation of the Rh/Al_2O_3 catalyst, studied by many others (including Li et al., [34]), is not observed. It is important to note, however, that that the temperatures experienced in UCAT testing are below those employed by Li et al. [34].

Given the differing relative performance strengths and prices of the PGMs they are often used in various combinations or blends in commercial TWC catalysts. As a simple first attempt at this strategy (i.e. to exploit the conversion properties of the 0.8% Pd/Al_2O_3 aerogel for CO and HC and of the 0.8% Rh/Al_2O_3 aerogel for NO) we prepared a physical mix (50/50 by volume) of the two aerogel types. This sample is

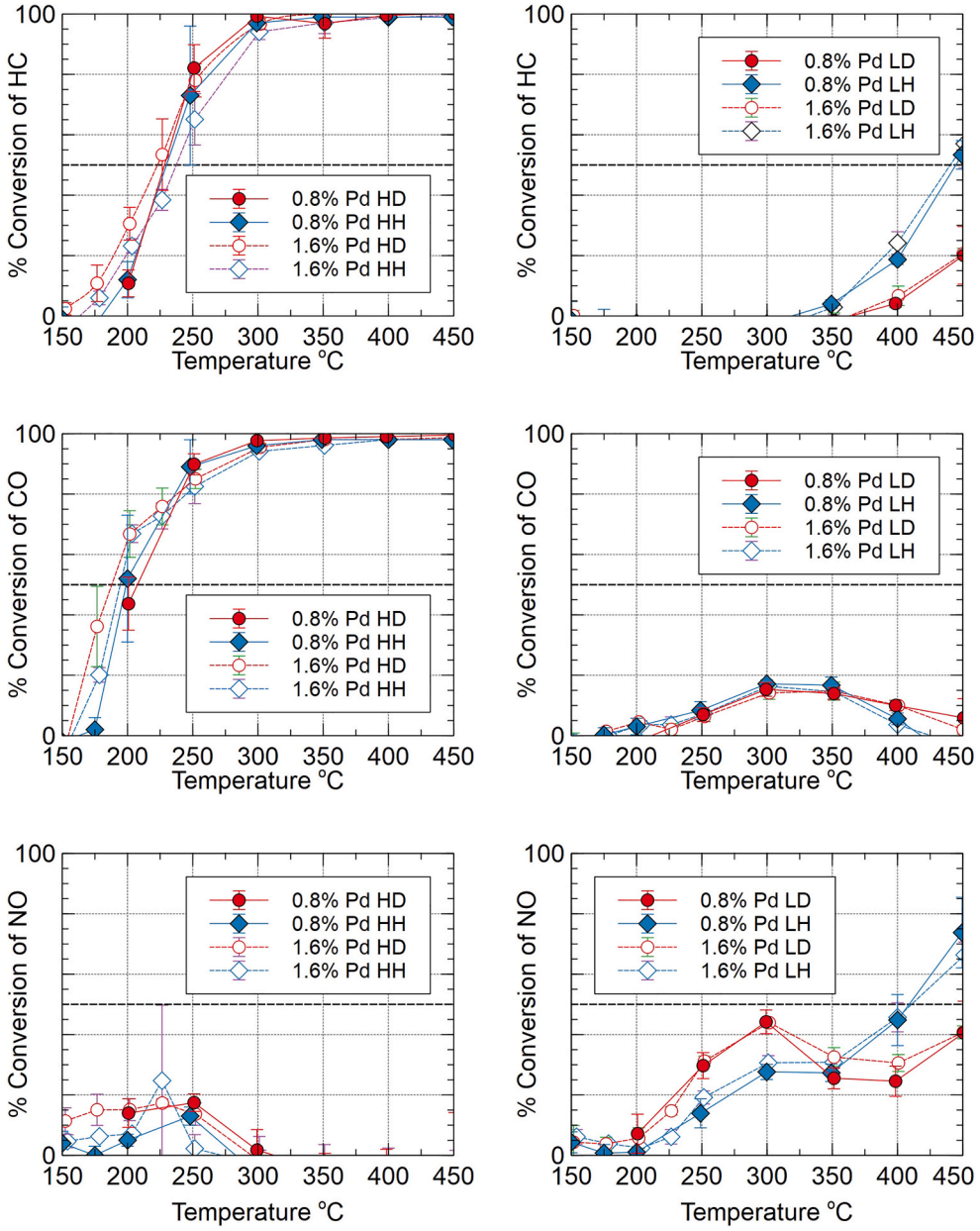

Fig. 4. Catalytic data for 0.8% Pd/Al_2O_3 and 1.6% Pd/Al_2O_3 aerogel under high O_2 (left column) and low O_2 (right column). Data collected under dry air conditions are indicated with a red circle and those measured under humid conditions are indicated with a blue diamond. Lines are provided as a guide to the eye. Error bars represent ±1 standard deviation in 2–4 tests. (For interpretation of the references to colour in this figure legend, the reader is referred to the web version of this article.)

designated 0.4%Rh:0.4%Pd/Al_2O_3. The catalytic testing results for the mix are plotted in Fig. 6. The light-off temperatures under high-O_2 conditions are 240–260 °C for HC and 220 °C for CO with little activity for HC and CO under low-O_2 conditions. Under low-O_2 conditions the NO light-off occurs at 260–270 °C. Within the uncertainty of the measurements, the performance of the mix is comparable to the better of the two components.

It should not be assumed that anything about this simple 50/50 mix of Pd and Rh aerogels is "optimal" for the TWC task, but it does demonstrate that (as expected) the strategy of mixing various PGMs is viable with PGM-doped aerogel catalysts, just as it is with other preparations. This also indicates that there is much to be done in future work with regards to studying optimal PGM ratios, exploring techniques such as staging different catalysts optimized for oxidation vs. reduction (also common in TWC design [35]), and exploring the use of "promoters" such as ceria to enhance the performance of the PGM package.

Table 2 summarizes light-off temperature results for the aerogels tested here and compares these data to those for an inert silica aerogel, a copper-alumina aerogel [10] and a sample cored from a commercially available catalytic converter (NAPA universal converter, part # 15037) tested in UCAT under the same conditions.

Interestingly, for the Pt-based aerogel, humidity enhances the high-O_2 oxidation of HC and CO (i.e. lower light-off) yet suppresses the low-O_2 reduction of NO. For the Pd-based aerogel, humidity does not affect the high-O_2 oxidation but does enhance the low-O_2 reduction of NO. For the Rh-based aerogel, humidity does not affect the high-O_2 oxidation of CO or the low-O_2 reduction of NO but does suppress the high-O_2 oxidation of HCs. The experiments presented here were designed to test whether PGM-containing alumina aerogels would act as TWCs, under the assumption that the reaction mechanisms would be comparable to those for PGMs on other, more conventional alumina supports. This study does not provide sufficient information to either confirm or refute the assumption regarding reaction mechanisms.

There is not much activity for oxidation of HC and CO under the low-O_2 conditions for any of the PGM-based aerogels although there is conversion of HCs at higher temperatures (400–450 °C) for the Pd- and Rh- based aerogels in a humid environment. It is possible that this increased destruction of HCs is caused via a steam reforming reaction,

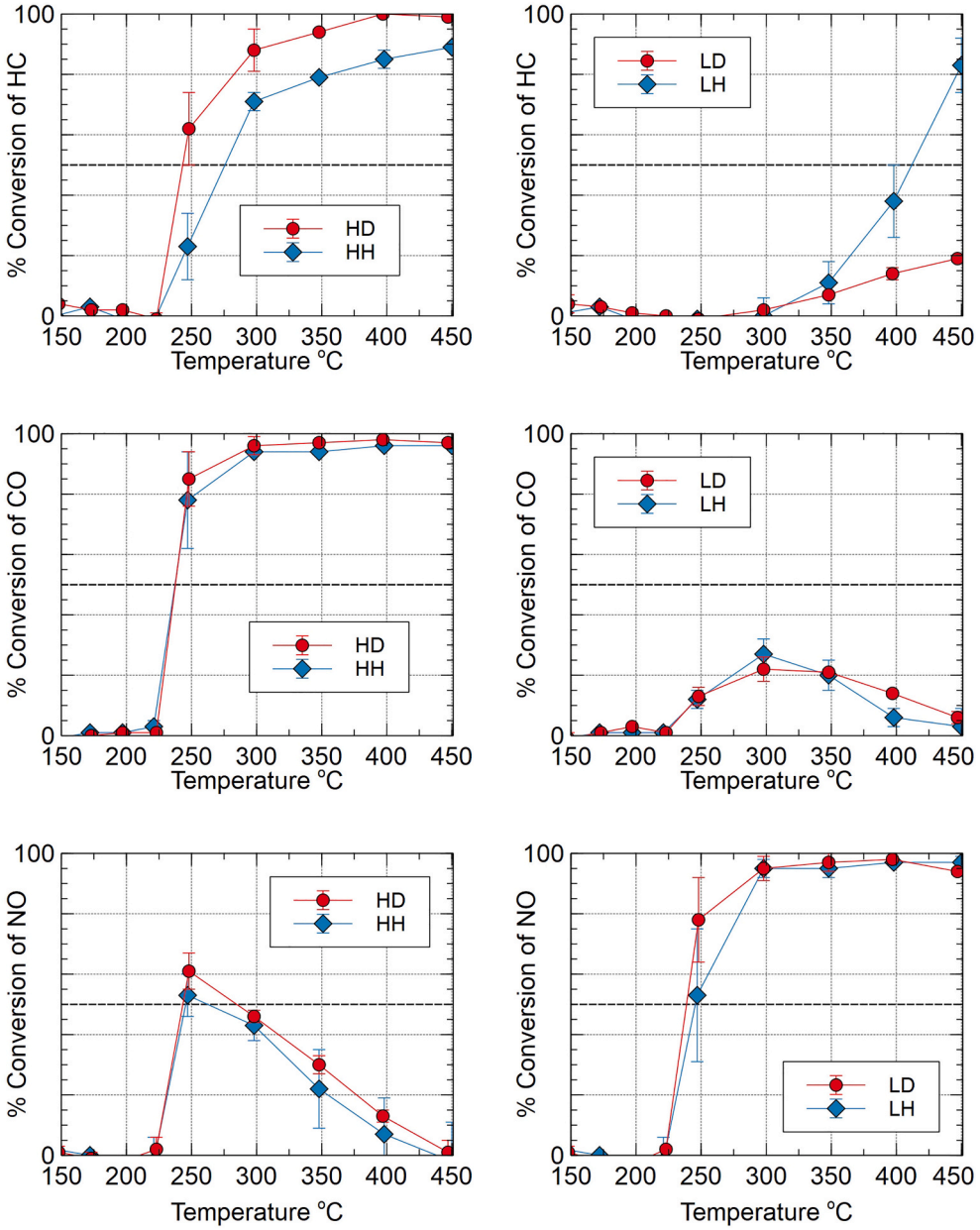

Fig. 5. Catalytic data for 0.8% Rh/Al_2O_3 aerogel under high O_2 (left column) and low O_2 (right column). Data collected under dry air conditions are indicated with a red circle and those measured under humid conditions are indicated with a blue diamond. Lines are provided as a guide to the eye. Error bars represent ±1 standard deviation in 2–3 tests. (For interpretation of the references to colour in this figure legend, the reader is referred to the web version of this article.)

which would be favored by increased concentrations of H_2O and increased temperature, but we have no evidence to directly support or reject this conjecture. Also, since the water gas shift reaction produces H_2, and since there is H_2 in the untreated test gas itself, it is possible that at least some of the NO which is eliminated might convert to NH_3, but again we have no direct evidence that this is occurring to a significant extent. Under high-O_2 conditions the 0.8% Rh/Al_2O_3, 0.8% Pd/Al_2O_3 and the physical mix of these aerogels show evidence of conversion of NO under both humid and dry conditions (see Figs. 4–6) that increases with temperature until about 250 °C and then decreases as the CO reaches 100% conversion. This is presumably due to the reduction of NO to N_2 by CO (although we note that the five-gas analyzers employed in UCAT do not detect nitrogen-containing products, which means that from the data obtainable we cannot rule out other possible reactions, including reduction to N_2O or oxidation to NO_2).

Beyond demonstrating that these particular PGM containing aerogels could be made via the RSCE process, and characterizing the resulting materials (including in terms of catalytic activity), one of our goals was to determine if they could be survivable under typical TWC conditions. Since some aerogels are known to be hydrophilic and/or are known to be damaged by the presence of water, we tested in both dry and humid conditions. As with other catalytic aerogels that we have tested under similar [10,11] and even more challenging conditions [12] we did not observe any gross dramatic degradation of the aerogels under humid or dry testing. This leads us to conclude that these catalytic aerogels can now be characterized as "potentially survivable" under automotive conditions. However, it must be noted that they have not been tested against the full array of challenges associated with automotive use, which include resisting various threats such as poisoning, high temperature deviations, thermal shock and thermal cycling, vibration loading, and long-term aging. We have also not yet investigated the hydrothermal stability of these materials; however, based on a slurry

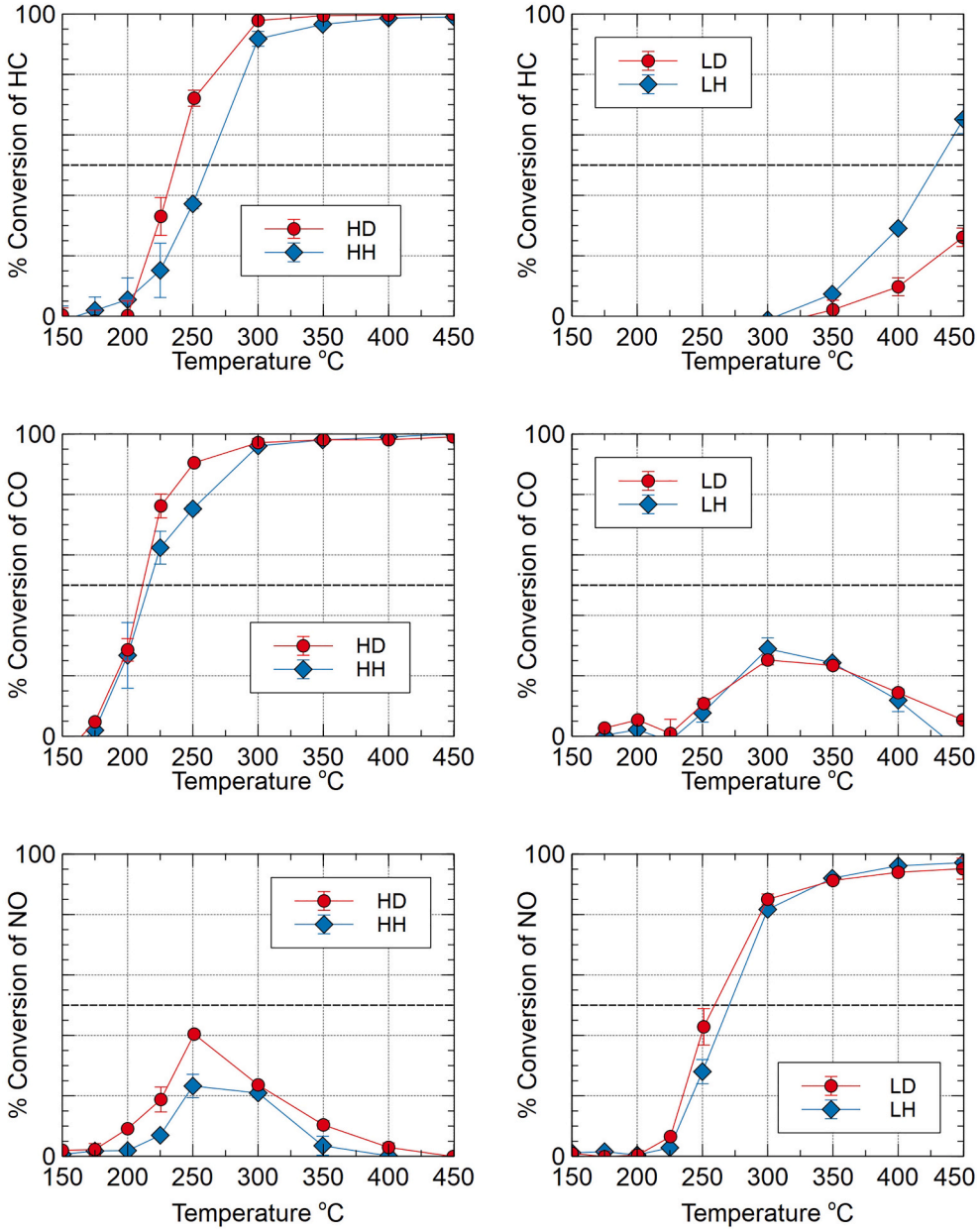

Fig. 6. Catalytic data for 0.4%Rh:0.4%Pd/Al_2O_3, a 50–50 (by volume) physical mix of 0.8% Pd/Al_2O_3 and 0.8% Rh/Al_2O_3 aerogel, under high O_2 (left column) and low O_2 (right column). Data collected under dry air conditions are indicated with a red circle and those measured under humid conditions are indicated with a blue diamond. Lines are provided as a guide to the eye. Error bars represent ±1 standard deviation in 2 tests. (For interpretation of the references to colour in this figure legend, the reader is referred to the web version of this article.)

processing study of copper-alumina aerogels [12] we have some confidence that they may perform well in this regard. The current data gives us confidence that future work aimed at answering those questions is warranted.

Another goal of this work is to determine whether the use of aerogel as a support material for PGMs allows for the use of lower amounts of PGMs than is required in traditional wash-coating materials. Unfortunately, it is difficult to make direct comparisons with literature reports of PGM-based three-way catalysts as there is a lack of clarity in the reporting of PGM loading and there are a range of simulant gas mixtures and space velocities used to characterize catalyst performance. For example, in a recent review article, Rood et al. [36] present light-off temperature results for a number of PGM-based catalysts. The reported loadings range from 0.5 to 3 wt% PGM in a range of wash-coat materials (alumina, ceria, etc.); however, it is unclear how the weight percent is calculated.

In the work presented here we calculated the weight percent of PGM based on the weight of the heat-treated aerogel sample (density ~ 0.1 g/mL). Conventional wash coats are significantly denser (4–7 g/mL). A more illuminating method for comparing our aerogel-based PGM catalyst is to look at PGM/volume data. Typical TWC PGM loading values are given at 1.8–2.8 g/L (50–80 g/ft^3) based, we believe, on the overall volume of the TWC honeycomb, sometimes called the "can volume" [37–39]. Such loadings are significantly higher than our PGM loadings of 0.08–0.16 g/L (2.3–4.6 g/ft^3). Additionally, we should note that the way we are reporting PGM mass volumetric loading is most broadly similar to reporting a "wash-coat loading" (i.e. grams of PGM per unit volume of finished wash-coat material). If we were to report our loading based on the mass of PGM within the total volume of the test cell (including air voids in the packed bed) then we would be reporting something more similar to a "can loading" which, numerically, would be significantly lower (since the can volume is necessarily larger than volume of wash-coat it contains).

Kang et al. [37] report results for commercial Pd-based catalysts with Pd loading of 20–230 g/ft^3 (0.7–8.1 g/L) (which we believe is based on can loading, and corresponds to 0.1–1.5 wt%) at a range of catalyst mileages from 4000 to 100,000 miles at a space velocity of 100,000 h^{-1}. The materials were tested in a simulated gas mix containing: 500 ppm

Table 2
Light-off temperatures* for aerogels tested under dry and humid conditions.

	HC		CO		NO	
Catalyst	High O_2	Low O_2	High O_2	Low O_2	High O_2	Low O_2
Silica	−−/−−	−−/−−	475/−−	−−/−−	−−/−−	−−/−−
CuAl	250/350	−−/500	220/270	−−/400	−−/−−	260/350
0.8% Pt/Al_2O_3	450/400	−−/−−	440/395	−−/−−	−−/−−	520/−−
0.8% Pd/Al_2O_3	225/225	−−/−−	205/200	−−/−−	−−/−−	460/410
1.6% Pd/Al_2O_3	220/230	450/450	190/200	−−/−−	−−/−−	460/410
0.8% Rh/Al_2O_3	245/275	−−/410	240/240	−−/−−	250/250	240/250
0.4%Rh: 0.4%Pd/Al_2O_3	240/260	−−/425	220/220	−−/−−	−−/−−	260/270
Commercial	220/210	−−/−−	190/210	−−/290	−−/−−	190/225

– indicates light-off not achieved by 600 °C.
* Values given in °C for dry (left)/humid (right) conditions. Due to the scatter in the data and the imprecision of the measurement of the light-off temperature the uncertainty is at least ±20 °C.

C_3H_6, 500 ppm NOx, 1% CO, 0.3% H_2, 10% H_2O, 10% CO_2 and 1% O_2 yielding an S value of 1.17 (slightly lean). For a loading of 80 g/ft^3 (2.8 g/L) at the lowest catalyst mileage (4000 miles) the light-off temperature for CO is 200 °C, for HC is 225 °C and for NO is 180 °C. Our 0.8% Pd/Al_2O_3 aerogel (0.08 g/L or 2.2 g/ft^3) under high-O_2 humid conditions show similar light-off temperatures of 200 and 225 °C for CO and HC respectively, at a PGM loading 36 times lower. Two caveats are important here. First the aerogel catalysts were tested under conditions significantly more favorable to oxidation (higher S value) and the comparative improvement in HC and CO conversion with the aerogel catalysts cannot be decoupled from or simply interpreted as "better performance" by the Pd in the aerogel. Second, the commercial catalysts have undergone some aging (in this case prepped at 600 °C for 16 h under periodic cycling in O_2 and CO) while our aerogel catalysis were heat treated at 800 °C for about 24 h in air. In addition, the Pd-based aerogels do not show much activity for the conversion of NO.

Although, as noted above, none of this comparison is perfect (different gas mixture and space velocity) the comparison does point to the potential for PGM-containing aerogels. Compared to Kang et al. we are able to achieve similar TWC performance with significantly lower PGM content. This result provides a clear direction for future work comparing *identical catalyst recipes*, differing only in if they are prepared as aerogels or in more conventional physical forms, under *identical gas and flow conditions* to more clearly determine the effects of aerogel processing, independent of other variables, on catalytic performance.

4. Conclusion

The remarkable properties of aerogels, including thermal stability, high surface area, and chemical tailorability, render them attractive for catalytic applications. Here we have presented the first method for making PGM-containing aerogels using a rapid supercritical extraction method, demonstrated that these materials function as three-way catalysts with low PGM loading under both dry and humid testing conditions, and observed that their catalytic performance remains stable through multiple testing cycles.

The aerogels examined were prepared with a relatively small amount of PGMs compared to conventional TWC catalysts, but they have not yet been optimized with regards to blend or total quantity of PGMs, and they do not include an oxygen storage component such as ceria (we do not expect the PGM/alumina aerogel itself to exhibit significant OSC capability, and we have demonstrated the ability to fabricate ceria-containing aerogels [13]). Likewise, they have not been exhaustively tested under every condition that they would experience in a real automotive application. For example, our testing does not perfectly mimic real automotive exhaust performance, which would include dithering, as well as various chemical (e.g. poisoning) and physical (e.g. overtemperature excursions) challenges. Nevertheless, preliminary measurements of our best performing aerogel catalyst, a mixture of Pd/Al_2O_3 and Rh/Al_2O_3 aerogel containing a relatively low amount of each PGM, demonstrated comparable catalytic performance to a sample of commercial TWC under the conditions tested. We have thus illustrated the promise of this research approach: using aerogel processing of essentially conventional TWC materials (i.e. alumina support, PGM active species) to enhance performance.

Beyond that, the RSCE fabrication approach for making aerogels is robust and potentially scalable and is only one of several potentially economical approaches to manufacturing aerogel catalysts at scale. Also, earlier research [12] provides evidence that aerogel catalysts can likely survive the types of conventional slurrying / washcoating processes used in TWC manufacture, easing the path to utilizing aerogel catalysts in TWCs. Taken together these facts indicate that further research into using aerogel PGM catalysts in TWCs is warranted.

Compliance with ethical standards

Conflict of interest: the authors declare that they have no competing interests.

CRediT authorship contribution statement

Ann M. Anderson: Conceptualization, Methodology, Investigation, Data curation, Writing – original draft, Writing – review & editing, Supervision, Project administration, Funding acquisition. **Bradford A. Bruno:** Conceptualization, Methodology, Investigation, Data curation, Writing – original draft, Writing – review & editing, Supervision, Project administration, Funding acquisition. **Joana Santos:** Writing – original draft, Investigation, Data curation. **Patrick J. Barry:** Investigation, Data curation. **Mary K. Carroll:** Conceptualization, Methodology, Investigation, Data curation, Writing – original draft, Writing – review & editing, Supervision, Project administration, Funding acquisition.

Declaration of Competing Interest

Ann M. Anderson, Bradford A Bruno, and Mary K. Mahony (Carroll) have patent #9,358,534 Catalyst, Catalytic Converter, And Method For The Production Thereof issued to Union College. Ann M. Anderson and Mary K. Mahony have patents #8,080,591 Method and Device for Fabricating Aerogels and Aerogel Monoliths Obtained Thereby issued to Union College and #7,384,988 Method and Device for Fabricating Aerogels and Aerogel Monoliths Obtained Thereby issued to Union College.

Data availability

Data will be made available on request.

Acknowledgements

This material is based upon work supported by the National Science

Foundation (NSF) [grants numbers IIP-1918217, IIP-1823899, DMR-1828144 and CBET-1228851]. We thank Anna Hoffman, Ethan Lampert and Sri Teja Mangu for help with the UCAT testing.

Appendix A. Supplementary data

Supplementary data to this article can be found online at https://doi.org/10.1016/j.catcom.2022.106547.

References

[1] W.A. Majewski, Catalytic coating & materials (2005). https://dieselnet.com/tech/cat_mat.php. (Accessed 28 October 2022).
[2] H. Nakayama, Y. Kanno, M. Nagata, X. Zheng, Development of TWC and PGM free catalyst combination as gasoline exhaust Aftertreatment, SAE Int. J. Engines 9 (2016), https://doi.org/10.4271/2016-01-2323.
[3] Y. Ren, D. Lou, P. Tan, Y. Zhang, X. Sun, Emission reduction characteristics of after-treatment system on natural gas engine: effects of platinum group metal loadings and ratios, J. Clean. Prod. 298 (2021), https://doi.org/10.1016/j.jclepro.2021.126833.
[4] T. Zheng, B. Lu, G. Harle, D. Yang, C. Wang, Y. Zhao, A comparative study of Rh-only, Pd-only and Pd/Rh catalysts, Appl. Catal. A Gen. 602 (2020), https://doi.org/10.1016/j.apcata.2020.117649.
[5] G.M. Pajonk, Some catalytic applications of aerogels for environmental purposes, Catal. Today 52 (1999) 3–13, https://doi.org/10.1016/S0920-5861(99)00057-7.
[6] G.M. Pajonk, Aerogel catalysts, Appl. Catal. 72 (1991) 217–266, https://doi.org/10.1016/0166-9834(91)85054-Y.
[7] H. Maleki, N. Hüsing, Current status, opportunities and challenges in catalytic and photocatalytic applications of aerogels: environmental protection aspects, Appl. Catal. B Environ. 221 (2018) 530–555, https://doi.org/10.1016/J.APCATB.2017.08.012.
[8] M.S. Bono Jr., A.M. Anderson, M.K. Carroll, Alumina aerogels prepared via rapid supercritical extraction, J. Sol-Gel Sci. Technol. 53 (2010), https://doi.org/10.1007/s10971-009-2080-5.
[9] S.J. Juhl, N.J.H. Dunn, M.K. Carroll, A.M. Anderson, B.A. Bruno, J.E. Madero, M. S. Bono, Epoxide-assisted alumina aerogels by rapid supercritical extraction, J. Non-Cryst. Solids 426 (2015), https://doi.org/10.1016/j.jnoncrysol.2015.06.030.
[10] Z.M. Tobin, L.F. Posada, A.M. Bechu, M.K. Carroll, R.M. Bouck, A.M. Anderson, B. A. Bruno, Preparation and characterization of copper-containing alumina and silica aerogels for catalytic applications, J. Sol-Gel Sci. Technol. 84 (2017), https://doi.org/10.1007/s10971-017-4425-9.
[11] A.M. Anderson, B.A. Bruno, F. Dilone, M.T. LaRosa, T.F. Andre, C. Avanessian, M. K. Carroll, Effect of copper loading in copper-alumina aerogels on three-way catalytic performance, Emiss. Control Sci. Technol. 6 (2020), https://doi.org/10.1007/s40825-020-00165-z.
[12] A.M. Anderson, B.A. Bruno, J. Santos, C. Avanessian, M.K. Carroll, Effect of slurry processing on the properties of catalytically active copper-alumina aerogel material for applications in three-way catalysis, J. Sol-Gel Sci. Technol. 102 (2022), https://doi.org/10.1007/s10971-022-05757-5.
[13] L.F. Posada, M.K. Carroll, A.M. Anderson, B.A. Bruno, Inclusion of ceria in alumina- and silica-based aerogels for catalytic applications, J. Supercrit. Fluids 152 (2019), https://doi.org/10.1016/j.supflu.2019.05.004.
[14] F.T. Fitzgerald, M.K. Carroll, A.M. Anderson, B.A. Bruno, Development of Catalytic Chromia-based Aerogels, Poster Number COLL 311 259th ACS Natl. Meet, 2020.
[15] Y. Jin, F. Chen, J. Wang, L. Guo, T. Jin, H. Liu, Lamellar platinum–rhodium aerogels with superior electrocatalytic performance for both hydrogen oxidation and evolution reaction in alkaline environment, J. Power Sources 435 (2019), https://doi.org/10.1016/j.jpowsour.2019.226798.
[16] C. Kwak, T.J. Park, D.J. Suh, Preferential oxidation of carbon monoxide in hydrogen-rich gas over platinum-cobalt-alumina aerogel catalysts, Chem. Eng. Sci. 60 (2005), https://doi.org/10.1016/j.ces.2004.07.126.
[17] B. Heinrichs, F. Noville, J.P. Pirard, Pd/SiO2-cogelled aerogel catalysts and impregnated aerogel and xerogel catalysts: synthesis and characterization, J. Catal. 170 (1997), https://doi.org/10.1006/jcat.1997.1772.
[18] L.M. Sanz-Moral, A. Romero, F. Holz, M. Rueda, A. Navarrete, A. Martín, Tuned Pd/SiO2 aerogel catalyst prepared by different synthesis techniques, J. Taiwan Inst. Chem. Eng. 65 (2016), https://doi.org/10.1016/j.jtice.2016.05.030.
[19] J. Choi, C.B. Shin, D.J. Suh, Co-promoted Pt catalysts supported on silica aerogel for preferential oxidation of CO, Catal. Commun. 9 (2008), https://doi.org/10.1016/j.catcom.2007.09.036.
[20] R.M. Al Soubaihi, K.M. Saoud, M.T.Z. Myint, M.A. Göthelid, J. Dutta, Co oxidation efficiency and hysteresis behavior over mesoporous pd/sio2 catalyst, Catalysts. 11 (2021), https://doi.org/10.3390/catal11010131.
[21] K.S. Morley, P. Licence, P.C. Marr, J.R. Hyde, P.D. Brown, R. Mokaya, Y. Xia, S. M. Howdle, Supercritical fluids: A route to palladium-aerogel nanocomposites, J. Mater. Chem. 14 (2004), https://doi.org/10.1039/b311065f.
[22] C. Hoang-Van, R. Harivololona, B. Pommier, Preparation of single and binary inorganic oxide aerogels and their use as supports for automotive palladium catalysts, Stud. Surf. Sci. Catal. 91 (1995), https://doi.org/10.1016/S0167-2991(06)81780-5.
[23] A.M. Anderson, E.A. Donlon, A.A. Forti, V.P. Silva, B.A. Bruno, M.K. Carroll, Synthesis and characterization of copper-nanoparticle-containing silica aerogel prepared via rapid supercritical extraction for applications in three-way catalysis, MRS Adv. (2017), https://doi.org/10.1557/adv.2017.343.
[24] T.F. Baumann, A.E. Gash, S.C. Chinn, A.M. Sawvel, R.S. Maxwell, J.H. Satcher, Synthesis of high-surface-area alumina aerogels without the use of alkoxide precursors, Chem. Mater. 17 (2005), https://doi.org/10.1021/cm048800m.
[25] B.M. Gauthier, S.D. Bakrania, A.M. Anderson, M.K. Carroll, A fast supercritical extraction technique for aerogel fabrication, J. Non-Cryst. Solids 350 (2004), https://doi.org/10.1016/j.jnoncrysol.2004.06.044.
[26] M.K. Carroll, A.M. Anderson, C.A. Gorka, Preparing silica aerogel monoliths via a rapid supercritical extraction method, J. Vis. Exp. (2014), https://doi.org/10.3791/51421.
[27] A.M. Anderson, B.A. Bruno, E.A. Donlon, L.F. Posada, M.K. Carroll, Fabrication and testing of catalytic aerogels prepared via rapid supercritical extraction, J. Vis. Exp. 2018 (2018), https://doi.org/10.3791/57075.
[28] G. Reichenauer, G.W. Scherer, Nitrogen sorption in aerogels, J. Non-Cryst. Solids 285 (2001) 167–174, https://doi.org/10.1016/S0022-3093(01)00449-5.
[29] B.A. Bruno, A.M. Anderson, M. Carroll, T. Swanton, P. Brockmann, T. Palace, I. A. Ramphal, Benchtop scale testing of aerogel catalysts: preliminary results, SAE Tech. Pap. (2016), https://doi.org/10.4271/2016-01-0920.
[30] K.G. Rappé, C. DiMaggio, J.A. Pihl, J.R. Theis, S.H. Oh, G.B. Fisher, J. Parks, V. G. Easterling, M. Yang, M.L. Stewart, K.C. Howden, Aftertreatment protocols for catalyst characterization and performance evaluation: low-temperature oxidation, storage, three-way, and NH 3 -SCR catalyst test protocols, Emiss. Control Sci. Technol. 52 (5) (2019) 183–214, https://doi.org/10.1007/S40825-019-00120-7.
[31] J.C. Schlatter, Water-gas shift and steam reforming reactions over a rhodium three-way catalyst, SAE Tech. Pap. (1978), https://doi.org/10.4271/780199.
[32] J.R. Theis, A. Getsoian, C. Lambert, The development of low temperature three-way catalysts for high efficiency gasoline Engines of the Future, SAE Int. J. Fuels Lubr. 10 (2017), https://doi.org/10.4271/2017-01-0918.
[33] C.-P. Hwang, C.-T. Yeh, Q. Zhu, Rhodium-oxide species formed on progressive oxidation of rhodium clusters dispersed on alumina, Catal. Today 51 (1999) 93–101, https://doi.org/10.1016/S0920-5861(99)00011-5.
[34] M. Li, X. Wu, Y. Cao, S. Liu, D. Weng, R. Ran, NO reduction by CO over Rh/Al2O3 and Rh/AlPO4 catalysts: metal–support interaction and thermal aging, J. Colloid Interface Sci. 408 (2013) 157–163, https://doi.org/10.1016/j.jcis.2013.07.023.
[35] R.M. Heck, R.J. Farrauto, Automobile exhaust catalysts, Appl. Catal. A Gen. 221 (2001) 443–457, https://doi.org/10.1016/S0926-860X(01)00818-3.
[36] S. Rood, S. Eslava, A. Manigrasso, C. Bannister, Recent advances in gasoline three-way catalyst formulation: a review, Proc. Inst. Mech. Eng. Part D J. Automob. Eng. 234 (2020), https://doi.org/10.1177/0954407019859822.
[37] S.B. Kang, I.-S. Nam, B.K. Cho, C.H. Kim, S.H. Oh, Universal activity function for predicting performance of Pd-based TWC as function of Pd loading and catalyst mileage, Chem. Eng. J. 259 (2015) 519–533, https://doi.org/10.1016/j.cej.2014.08.017.
[38] S.B. Kang, J. Bin Lim, D. Jo, I.-S. Nam, B.K. Cho, S.B. Hong, C.H. Kim, S.H. Oh, Ostwald-ripening sintering kinetics of Pd-based three-way catalyst: importance of initial particle size of Pd, Chem. Eng. J. 316 (2017) 631–644, https://doi.org/10.1016/j.cej.2017.01.136.
[39] J. Cooper, J. Beecham, A study of platinum group metals in three-way autocatalysts, Platin. Met. Rev. 57 (2013) 281–288, https://doi.org/10.1595/147106713X671457.